

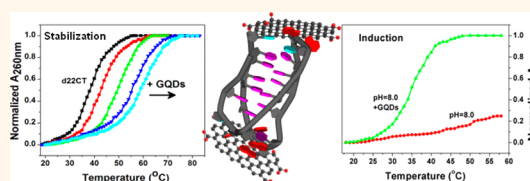
# Stabilization and Induction of Oligonucleotide i-Motif Structure *via* Graphene Quantum Dots

Xin Chen,<sup>†,§</sup> Xuejiao Zhou,<sup>‡,§</sup> Ting Han,<sup>‡</sup> Jiaying Wu,<sup>†</sup> Jingyan Zhang,<sup>†,\*</sup> and Shouwu Guo<sup>‡,\*</sup>

<sup>†</sup>Shanghai Key Laboratory of New Drug Design, State Key Laboratory of Bioreactor Engineering, School of Pharmacy, East China University of Science and Technology, Shanghai, 200237, People's Republic of China and <sup>‡</sup>Key Laboratory of Thin Film and Microfabrication of the Ministry of Education, Research Institute of Micro/Nano Science and Technology, Shanghai Jiao Tong University, Shanghai, 200240, People's Republic of China, <sup>§</sup>These authors contributed to this work equally.

**ABSTRACT** DNA i-motif structures have been found in telomeric, centromeric DNA and many in the promoter region of oncogenes; thus they might be attractive targets for gene-regulation processes and anticancer therapeutics. We demonstrate in this work that i-motif structures can be stabilized by graphene quantum dots (GQDs) under acidic conditions, and more importantly GQDs can promote the formation of the i-motif structure under alkaline or physiological conditions. We

illustrate that the GQDs stabilize the i-motif structure through end-stacking of the bases at its loop regions, thus reducing its solvent-accessible area. Under physiological or alkaline conditions, the end-stacking of GQDs on the unfolded structure shifts the equilibrium between the i-motif and unfolded structure toward the i-motif structure, thus promoting its formation. The possibility of fine-tuning the stability of the i-motif and inducing its formation would make GQDs useful in gene regulation and oligonucleotide-based therapeutics.



**KEYWORDS:** graphene quantum dots · i-motif · stabilization · induction · end-stacking

Human telomeric DNA is composed of multiple repeats of TTAGGG on one strand and CCCTAA on the other. The G-rich strand can form a four-stranded G-quadruplex consisting of G-quartets, whereas its complementary C-rich strand may adopt i-motif structures with intercalated C:C<sup>+</sup> base pairs.<sup>1,2</sup> Folding a telomeric G-rich strand into a G-quadruplex has been found to inhibit the activity of telomerase; thus it was deduced that the stabilization of G-quadruplexes can then be considered as a strategy to achieve antitumor activity.<sup>3–5</sup> The C-rich quartet, the i-motif, is a relatively young noncanonical DNA structure compared with the G-quadruplex. However, C-rich sequences have also been found present in or near the regulatory regions of more than 40% of all genes, especially in the promoter region of oncogenes.<sup>6,7</sup> For example, a C-rich i-motif structure has been found in the VEGF, c-Myc, and Rb promoter regions.<sup>8</sup> i-Motif DNA thus has been an emerging research topic because it might be an attractive drug target for anticancer drug design and for gene-regulation processes.<sup>9</sup> To this end, it is important to identify various molecules that

can modulate the stability of i-motif structures or promote their formation in order to fine-tune their properties. Notably, many small molecules can stabilize the G-quadruplex, but few bind to the i-motif. Cationic porphyrins and acridine dimers were reported to promote the formation of the G-rich and C-rich DNA quartets and stabilize them by binding externally.<sup>10–12</sup> Qu and co-workers recently reported carboxyl-modified single-walled carbon nanotubes (SWNTs) could selectively induce human telomeric i-motif formation by shifting the pK<sub>a</sub> of C:C<sup>+</sup> base pairs.<sup>13</sup> Except for SWNTs, small molecules with a large flat aromatic surface or a planar and circular structure can bind to the i-motif or G-quadruplex. In fact, these planar small molecules are structurally similar to DNA intercalators.<sup>14</sup> We have previously demonstrated that graphene oxide sheets, which have single atomic layered structure,<sup>15</sup> can intercalate with DNA plasmids. Combining with copper ions, the supercoiled DNA can be cleaved into nicked DNA by graphene oxide, which is analogous to DNA intercalators.<sup>16</sup> Recently we observed that graphene oxide could enhance the nuclease

\* Address correspondence to jyzhang@ecust.edu.cn, swguo@sjtu.edu.cn.

Received for review October 9, 2012 and accepted December 17, 2012.

Published online December 17, 2012 10.1021/nn304673a

© 2012 American Chemical Society

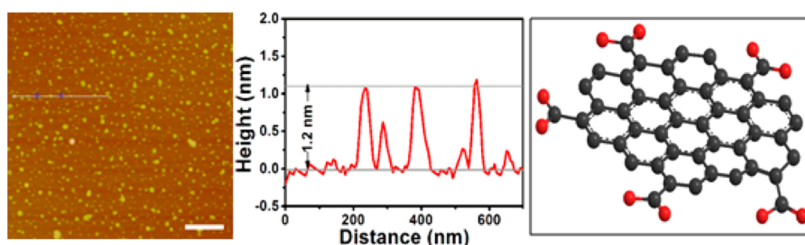


**Figure 1.** AFM image, height profile, and schematic structure of the GQDs used in the present work. Scale bar equals 500 nm. Red balls in GQD chemical structure are oxygen atoms; dark gray balls are carbon atoms.

activity and cytotoxicity of small DNA cleaving agents.<sup>17</sup> Additionally, we also illustrated that graphene oxide sheets with small lateral size exhibited higher DNA cleavage activity in the presence of copper ions.<sup>18</sup> These results indicated that the planar structure and lateral dimension of the graphene oxide sheets play a critical role in their interaction with DNA molecules.

On the basis of these results, in this work we study the interaction between graphene quantum dots (GQDs) with peripheral carboxylic acid groups and i-motif DNA. GQDs are graphene sheets with lateral dimensions less than 100 nm and possess numerous novel chemical/physical properties.<sup>18,19</sup> Due to the unique single atomic-layered structural motif, intrinsic properties, and small lateral dimension, GQDs are promising in cellular imaging, drug delivery, and other functions in biological systems.<sup>18,20,21</sup> The human telomeric i-motif (5'-CCCTAACCCCTAACCCCTAACCCCT-3', abbreviated as d22CT, where C, T, and A denote cytosine, thymine, and adenine moieties, respectively) has four C:C<sup>+</sup> base pairs that intercalate with opposite polarity, forming four chains and three short TAA loops. The crystal structure of i-motif d22CT showed that it is a compact structure with two wide grooves and two narrow grooves. It twists in a right-handed manner, and the specific geometry causes a closer stacking of the bases than that in a regular DNA helix.<sup>22</sup> Another i-motif structure of oncogene c-Myc used in this work assumes a similar conformation,<sup>8,23</sup> it has three longer loops between six intercalated C:C<sup>+</sup> base pairs (5'-TCCCCACCTCCCCACCCCTCCCCACCCCT-3', abbreviated as c-Myc), as schematically shown in Figure S1. Using a variety of spectroscopic techniques and gel electrophoresis, we found that GQDs can selectively stabilize i-motif structures under acidic conditions and induce the i-motif structure formation at physiological or alkaline pH *via* end-stacking on the bases of i-motif loops. The possibility of fine-tuning the i-motif stability and inducing i-motif formation would make GQDs useful in gene regulation and oligonucleotide-based therapeutics.

## RESULTS AND DISCUSSION

**GQDs Can Stabilize the i-Motif Structure and Induce i-Motif Structure Formation.** The GQDs were prepared through the photo-Fenton reaction of graphene oxide and fully characterized as described in our recent work.<sup>18</sup> Figure 1

shows the atomic force microscopy (AFM) images of the GQDs used in this work. The C/O atomic ratio of the GQDs is 1.26, which is much lower than that of GO,<sup>15</sup> indicating that they are enriched with carboxyl groups. The zeta potential of the GQDs is more positive than that of GO, because most surface functional groups of the GO were converted into carboxylic groups during oxidation (see Figure S2).<sup>18</sup> GQDs are on average ~40 nm in lateral size with peripheral carboxylic acid groups. The effect of GQDs on the i-motif structures is first evaluated by measuring the melting temperature ( $T_m$ ) in the presence of various amounts of GQDs by UV thermal denaturation. Because the stability of the i-motif is significantly affected by the protonation state of cytosine bases in the strand,<sup>2</sup> to exclude the effect of the acidity of the GQD samples, the GQD samples were dialyzed against Milli Q water and the pH of the GQD aqueous suspension was kept close to 7. Figure 2a shows that the  $T_m$  of the d22CT increased with an increase in the GQD concentration. The  $T_m$  of d22CT at pH 5.5 increased from 38 to 42 °C in the presence of 2.5  $\mu\text{g mL}^{-1}$  GQDs, and the  $T_m$  increased to 58 °C when the GQD concentration was 20  $\mu\text{g mL}^{-1}$ . Such a large  $\Delta T_m$  indicates that GQDs can stabilize the d22CT. Similar experiments were carried out with i-motif c-Myc under the same conditions; a  $\Delta T_m$  of 16 °C was observed (Figure 2b). The effect of GQDs on the stability of the i-motif conformation was also monitored using circular dichroism (CD) spectroscopy. Under acidic conditions (pH 5.5), the typical CD spectrum of the i-motif d22CT usually exhibits a positive band at 288 nm and a negative band at 256 nm.<sup>24</sup> Similarly, the CD spectrum of the c-Myc i-motif has a positive band at 285 nm and a negative band at 260 nm. Figure S4 shows that the CD spectrum of the i-motif d22CT in the presence of GQDs is unchanged and the i-motif structure is maintained.

To confirm the stabilization of the i-motif structure by GQDs, experiments with the random coil d22CT that exists at pH 8 were also carried out. Figure 3a shows the pH dependence of the typical CD spectra of d22CT. At pH 5.5, the d22CT structure exhibits its typical i-motif spectrum. As the pH is increased, a shift from 287 to 265 nm was observed, and the magnitude of the ellipticity at 287 nm decreased sharply, eventually leading to a characteristic spectrum of random coil

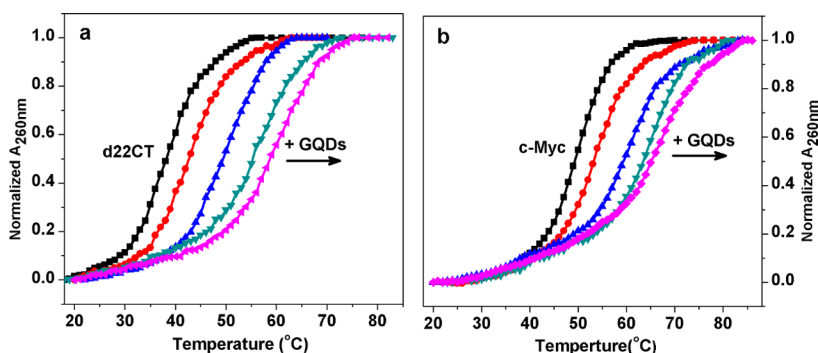


Figure 2. GQDs could stabilize the i-motif structure. UV melting curves of the i-motif d22CT (a) and c-Myc (b) in the presence of various amounts of GQDs: 2.5 (red), 5 (blue), 10 (green), 20  $\mu\text{g mL}^{-1}$  (magenta) in pH 5.5 cacodylic buffer (0.1 mM cacodylic acid/sodium cacodylate/100 mM NaCl). Black lines in each figure are the i-motifs without GQDs.

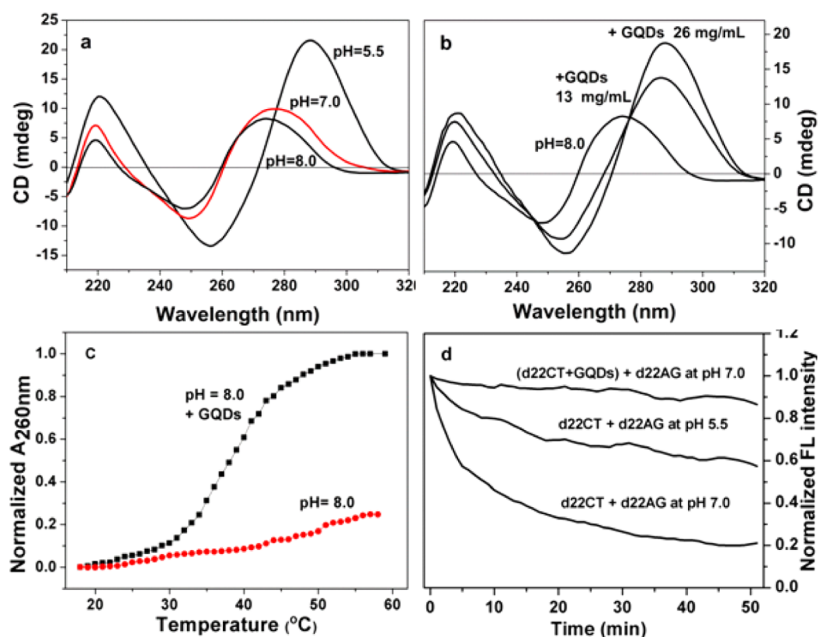
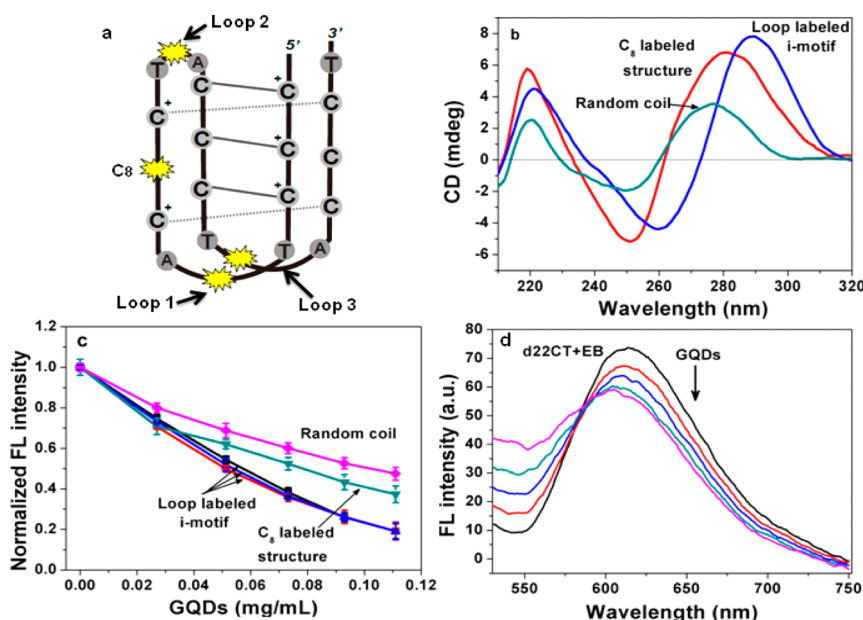


Figure 3. GQDs induce human telomeric i-motif structure formation. (a) CD spectra of the d22CT at pH 5.5, 7.0, and 8.0 in cacodylic buffer (0.1 mM cacodylic acid/sodium cacodylate/100 mM NaCl). (b) CD spectra of the d22CT at pH 8.0 in the presence of 0, 13, and 26  $\mu\text{g mL}^{-1}$  GQDs. (c) UV melting profiles of the d22CT in the absence or presence of GQDs (30  $\mu\text{g mL}^{-1}$ ) in the cacodylic buffer at pH 8. (d) Effect of the induced i-motif structure on G/C helix formation. Fluorescence emission changes at 370 nm of the C-rich single strand (2-*Ap* containing sequence d(CCCTAACCCCTAACCCT(2-*Ap*))ACCCT), 1  $\mu\text{M}$  with the complementary strand d(AGGGTTAGGGTTAGGGTTAGGG), d22AG.

structure, which has peaks at 248 and 274 nm.<sup>25</sup> In the presence of GQDs, the CD spectrum of the random coil d22CT (pH = 8) evolved into a typical i-motif conformation spectrum (Figure 3b). Figure S4b shows that a similar phenomenon occurred with a c-Myc random coil structure in the presence of GQDs. The CD measurement with GQDs was also carried out at pH 7, and the same result was obtained. These results indicate that GQDs could induce i-motif structure formation in neutral and alkaline conditions. To verify this result, <sup>1</sup>H NMR spectra of three samples, i-motif d22CT, random coil d22CT, and random coil d22CT with GQDs, were acquired (Figure S5). Although the signals were weak, chemical shifts at 15–16 ppm for the imino protons in C:C<sup>+</sup> of the i-motif were observed in the samples of d22CT i-motif<sup>1</sup> and d22CT random coil with GQDs, but

not in the random coil d22CT sample, implying that the i-motif structure was formed in the presence of GQDs at pH = 8.0, consistent with the CD data. The induction ability of GQDs is also solidified by the  $T_m$  change of the d22CT at pH 8.0 in the presence of GQDs. Figure 3c shows that at pH 8 d22CT is a random coil, thus exhibiting a flat melting profile as a function of temperature. In contrast, in the presence of GQDs, the melting curve exhibits a typical melting transition that is similar to the i-motif structure (pH 5.5).<sup>24</sup> A similar result was also obtained for c-Myc at pH 8 (Figure S4c).

To corroborate the induction ability of GQDs, a duplex competitive gel shift assay was performed with d22CT and its complementary G-rich strand d22AG. Figure S6 shows the native PAGE images of the d22CT strand and its complementary strand d22AG in the



**Figure 4.** (a) Four 2-Ap-labeled sites in d22CT, respectively. (b) CD spectra of the 2-Ap-labeled samples. The random coil is the loop3-labeled sample at pH 8.0. (c) Fluorescence intensity changes of the 2-Ap-labeled d22CT structures in the presence of GQDs. (d) Interaction of the d22CT i-motif with ethidium bromide (EB) and GQDs.

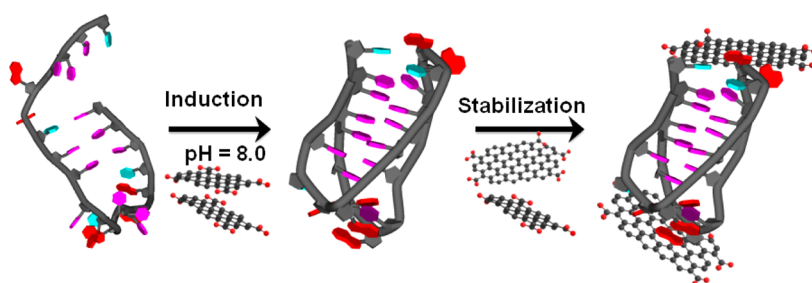
presence and absence of GQDs. Comparing to the duplex of d22CT and d22AG at pH 7.0 (lane 4), in the presence of GQDs at pH 7.0, in addition to the C/G duplex band, two bands assigned for i-motif structures were observed (lane 5).<sup>26</sup> The observation of the i-motif bands indicates that an i-motif structure was formed in the presence of GQDs, and the as-formed i-motif competed with the helix formation. A similar observation was reported using SWNTs also.<sup>13</sup> It was also reported that the C60/i-motif DNA hybrid could shift the conformational equilibrium between the i-motif and the duplex structure due to hydrophobic interactions introduced by C60.<sup>27</sup>

GQDs induce i-motif formation, which was further established by the fluorescence quenching experiments with 2-amniopurine (2-Ap)-labeled d22CT (CCCTAACCTAACCT(2-Ap)ACCT, d22CT(2-Ap)).<sup>28</sup> 2-Ap is a fluorescence adenine isomer that is able to form a Watson–Crick base pair with thymine and thus would not disturb the i-motif structure (Figure S7). The fluorescence emission of the i-motif d22CT(2-Ap) at pH 5.5 was only moderately quenched by its complementary strand d22AG because the i-motif structure affects its coupling with the complementary strand.<sup>29</sup> At pH 7.0, d22CT(2-Ap) is a partially unfolded i-motif structure, and it can form relatively easily a duplex with its complementary strand; thus the fluorescence of d22CT(2-Ap) was quenched dramatically (Figure 3d). In contrast, in the presence of GQDs under identical conditions, the fluorescence emission of the d22CT(2-Ap) is barely quenched, indicating that helix formation did not occur. This is expected because the GQDs promoted the formation of i-motif d22CT(2-Ap) and stabilized it; thus it cannot couple with its complementary strand. Collectively, these findings concur that the

GQDs not only stabilize the i-motif structure but also can promote its formation in neutral or alkaline conditions.

**Mechanism of Stabilization and Induction by GQDs.** A key issue that needs to be illustrated is how the GQDs interact with d22CT to induce i-motif structure formation and to stabilize it. It was reported that the fullerenes-attached i-motif could interact hydrophobically with the internal TAA loop in the DNA strand, resulting in an equilibrium shift between helix and i-motif.<sup>27</sup> It was also proposed that the carboxyl-modified SWNTs can stabilize and induce i-motif formation by lowering the  $pK_a$  of the C:C<sup>+</sup> base pairs through selectively interacting with loop1 of the d22CT.<sup>13</sup>

To define the binding site of GQDs at the i-motif, three adenosines at the three loops and the eighth cytosine from the 5' terminus of the d22CT were labeled with 2-Ap, respectively, as schematically shown in Figure 4a. The labeled samples were first subjected to CD measurements to examine whether the i-motif structure is disrupted. We found that labeling at the loops does not disturb the i-motif structure (Figure S7), but labeling at the eighth position results in a partially unfolded structure (Figure 4b). Figure 4c shows the profiles of the normalized fluorescence intensity of these samples *versus* the GQD concentration. With the GQD concentration increasing, the fluorescence intensity decreased equally for three loop-labeled samples, suggesting that GQDs interact with the d22CT i-motif at the three loop positions equally. The result also indicates that GQDs possibly assume an end-stacking interaction mode to bind to the i-motif structure. To exclude that the interaction of GQDs with the i-motif is a nonspecific physical adsorption, 2-Ap-labeled random coil d22CT was examined. Note that the fluorescence of the 2-Ap-labeled random coil d22CT alone is weaker



**Scheme 1.** Proposed mechanism of the stabilization and induction of the i-motif structure by GQDs. Folded i-motif structure is generated from the PDB file (PDB id: 1EL2). Pink, cytosine; blue, thymidine; red, adenosine. Red balls in GQDs are oxygen atoms; gray balls are carbon atoms.

than that of the 2-Ap-labeled i-motif, possibly because the fluorescence of 2-Ap is easily quenched in a random coil conformation, as it is more exposed.<sup>29</sup> Interestingly, the normalized fluorescence intensity of the labeled random coil drops much slower than that of the loop-labeled i-motif with the increase of GQD concentration. These results reveal that GQDs interact more strongly with the i-motif at loop positions. Actually, it was reported earlier that SWNTs could interact with loop1 of the d22CT preferentially, deduced from a slight decrease in the fluorescence intensity of the loop1-labeled i-motif.<sup>13</sup> Notably, the fluorescence quenching of the loop-labeled d22CT i-motif by GQDs is 4-fold stronger than that by SWNTs, implying that GQDs stabilize the i-motif rather through stacking on the loops than lowering the  $pK_a$  of the C:C<sup>+</sup> base pairs, as proposed for SWNTs. To reaffirm the GQDs' end-stacking binding mode, the eighth cytosine-labeled d22CT (C<sub>8</sub>-labeled structure in Figure 4b and c) was prepared. Intriguingly, the fluorescence quench profile by GQDs of this partially unfolded structure (Figure 4b) is in between that of the i-motif and random coil. These findings suggested that GQDs preferentially stack on the loops of the i-motif structure.

The other possible binding mode of GQDs to the i-motif is intercalation. We previously showed that graphene oxides could intercalate in a DNA duplex by CD and the fluorescence replacing method using ethidium bromide (EB).<sup>16</sup> In the case of the i-motif structure, the fluorescence emission of EB was also enhanced in the presence of d22CT, but by only about 1.5-fold, which is much lower than that of a DNA duplex (20-fold), implying that EB externally stacks on the i-motif,<sup>30</sup> similar to the binding mode of thiazole orange, another generally used DNA intercalator.<sup>31</sup> Introducing GQDs to the mixture of d22CT/EB, the fluorescence intensity decreased as the amount of GQDs increased, as shown in Figure 4d. This fluorescence quenching could be caused either by the GQDs binding to EB molecules that stacked on the i-motif or by the GQDs binding to the i-motif directly. To differentiate these two cases, fluorescence of the GQDs and d22CT i-motif mixture was first measured, and almost no fluorescence signal was detected. Fluorescence

intensity of EB alone was also recorded in the presence of various amounts of GQDs. As shown in Figure S8, in the presence of GQDs, the fluorescence intensity of EB itself can be quenched, which is consistent with the fluorescence quench ability of graphene oxide reported in the literature.<sup>32</sup> Notably, in the presence of GQDs, the decrease in the amplitude of fluorescence intensity of EB alone is similar to that of EB/d22CT, implying that GQDs quenched the fluorescence of EB/d22CT by stacking on the EB. The result further supports that GQDs interact with the i-motif by end-stacking instead of intercalation. Comparing to the double helix, the end-stacking mode is expected, because the distance between two adjacent base pairs in the i-motif is smaller (3.1 Å vs 3.4 Å in the helix). In addition, in the four-stranded intercalated i-motif structure, neighboring C:C<sup>+</sup> base pairs from intercalated duplexes are arranged in a way that no overlap exists between their six-membered aromatic ring systems.<sup>22</sup> Such a structural arrangement is not favorable for GQD intercalation.

Taking these results together, we believe that GQDs tend to end-stack on the three loops of the i-motif, as schematically shown in Scheme 1. At the three loop positions, adenines and thymidines that have heterocycles can stack with GQDs through  $\pi$ - $\pi$  stacking, because they are fully exposed to solvent. It has been generally believed that molecular ion-dipole interactions, sugar-sugar contacts, dipole-dipole interactions, and interstrand C-H-O hydrogen bonds are factors that determine the stability of the i-motif.<sup>33,34</sup> The interaction of GQDs with the i-motif does not seem to be relevant to these stability-related factors. However, the stacking between adenines or thymidines of the i-motif with GQDs decreases its terminal base-pair solvent-accessible area,<sup>6</sup> thus dramatically increasing its stability. i-Motif DNA is found to be structurally dynamic over a wide range of pH. The classical i-motif structures are predominant in the pH range of 4.2–5.2, whereas partially unfolded and single-stranded structures are the most significant species in solution at pH values higher and lower than that range, respectively.<sup>25,35,36</sup> There are equilibria among these multiple conformations. At pH 8, the dominant structure of d22CT is an unfolded

conformation, and a small amount of folded i-motif structure also exists. In the presence of GQDs, the stability of the i-motif species is improved, which will shift the equilibrium from unfolded structure to the folded i-motif structure and eventually induce the formation of the i-motif structure.<sup>25</sup> Additionally, given that most of the surface of the GQDs is hydrophobic, while the peripheral region is negative due to the carboxylic groups, repulsive interaction between GQDs and negatively charged phosphate groups of d22CT should be favorable to the base-pair formation of d22CT itself also. Interestingly, we did not observe any stabilization or induction ability of GQDs to the G-quadruplex under similar conditions (data not shown). It seems an optimized combination of size and structure of both GQDs and the i-motif results in selectivity in their interaction.

## CONCLUSIONS

We demonstrate that GQDs can stabilize i-motif structures in acidic conditions and promote its formation in

neutral or alkaline conditions. The stabilization and induction mechanism of GQDs are systematically studied by CD, fluorescence spectroscopy, and melting temperature. We found that the GQDs stabilize the i-motif structure through end-stacking on its bases at the loops, thus reducing the solvent-accessible area of the i-motif. In alkaline conditions, the stack of GQDs on the i-motif structure shifts the balance between the i-motif and unfolded structure by stabilizing the i-motif structure, eventually promoting the formation of the i-motif. The interaction mode of GQDs with the i-motif is different from that of SWNTs, possibly because they have different sizes and structural conformations. The interaction mode is also different from the graphene oxides with DNA duplex, owing to the shorter distance between the base pairs and weaker base-pair stacking in the i-motif structure. The abilities to tune the i-motif stability and to induce i-motif formation would allow GQDs to find potential applications in gene regulation processes and anticancer therapeutics.

## MATERIALS AND METHODS

**Materials.** GQDs were prepared through photo-Fenton reactions of graphene oxide and were generated as described in our previous work. The reaction of graphene oxide was carried out in a photoreactor equipped with irradiation lamps having different emission wavelengths and powers (Bilon, Shanghai). The reaction is carried out in a 40 mL quartz tube with vigorous stirring. The lamps were placed inside a cylindrical Pyrex tube cooled by circulating water. The typical reaction mixture is composed of graphene oxide and Fenton reagent, FeCl<sub>3</sub> and H<sub>2</sub>O<sub>2</sub>. The reaction products were dialyzed in ultrapure water for two days to remove reactants and small product molecules. The generated GQDs were characterized by AFM, XPS, and FT-IR, as we described in our previous work.

HPLC-purified human telomeric DNA, 5'-CCCTAACCTAACCTAACCT-3' (d22CT), its corresponding complementary strand, 5'-AGGGTTAGGGTTAGGGTTAGGG-3' (d22AG), c-Myc 5'-TCCCCACCTCCCCACCTCCCCACCT-3', 2-aminopurine (2-Ap)-labeled d22CT, 5'-CCCT(2-Ap)ACCCTAACCTAACCT-3', 5'-CCCTAACCT(2-Ap)ACCCTAACCT-3', and 5'-CCCTAACCTAACCT(2-Ap)ACCCT-3' were purchased from Sangon (Shanghai, China) and used without further purification. Concentrations of these oligomers were determined by measuring their absorbance at 260 nm after melting. i-Motif and G-quadruplex samples were prepared as follows: The oligonucleotide samples were dissolved in 0.1 mM cacodylic acid/sodium cacodylate/100 mM NaCl buffer, heated to 90 °C for 8 min, gently cooled to room temperature, and then incubated at 4 °C overnight.

**Methods.** Melting curves of the oligonucleotides (each strand concentration is 1.5 μM) were recorded by a Cary 50 UV/vis spectrophotometer equipped with a Peltier temperature control accessory. Absorbance changes at either 260 nm (i-motif) or 295 nm (G-quadruplex) versus temperature were collected at a heating rate of 1 °C/min. The melting curves were plotted using the normalized absorbance versus temperature.

The CD spectra were recorded on a Chirascan spectropolarimeter (Applied Photophysics, UK) equipped with a temperature-controlled water bath. The optical chamber of the CD spectrometer was deoxygenated with dry purified nitrogen for 30 min before use, and the nitrogen atmosphere was maintained during the experiments. Samples were dissolved in the buffers and loaded into a 10 mm quartz cuvette. Spectra were recorded from 200 to 320 nm with 1 nm bandwidth and 0.5 s

collection time per point at 20 °C; each spectrum is the average of three scans.

Native polyacrylamide gel electrophoresis (20%) was carried out in 45 mM Tris-borate buffer. Gel electrophoresis was run at 4 °C for 2 h under 120 V. The gels were silver-stained and visualized by a Tanon-2500 gel imaging system. The G/C duplex was formed by mixing an equal molar concentration of d22CT and d22AG at 4 °C overnight in 0.1 mM cacodylic acid/sodium cacodylate/100 mM NaCl buffer (pH 7.0).

Fluorescence measurements were carried out on a Cary Eclipse spectrofluorometer (Varian, USA) at 20 °C. Fluorescence spectra of 2-AP-labeled i-motif DNA were measured by using an excitation wavelength of 305 nm and emission at 370 nm in the absence or presence of different amounts of GQDs. For the experiment with EB, fluorescence emission was recorded from 530 to 750 nm with an excitation wavelength of 480 nm.

<sup>1</sup>H NMR spectra were carried out on a 500 MHz Bruker Avance spectrometer equipped with a 5 mm PABBO BB probe. A total of 1024 scans at 291 K were acquired for each spectrum with a relaxation delay of 4 s. Individual DNA samples were used at different pH conditions in the absence or presence of GQDs. DNA concentration was 0.2 mM in the strands.

**Conflict of Interest:** The authors declare no competing financial interest.

**Supporting Information Available:** Schematic diagrams of the i-motif structures and of GQDs inducing c-Myc i-motif structure formation, <sup>1</sup>H NMR spectra of the d22CT at different pH and with GQDs at pH 8, images of the native PAGE of the d22CT i-motif and its complementary strand d22AG in the presence and absence of GQDs, CD spectra of the i-motifs that were labeled with 2-Ap and of GQDs quenching the fluorescence of EB (5 μM). This material is available free of charge via the Internet at <http://pubs.acs.org>.

**Acknowledgment.** This work was financially supported by the National Science Foundation of China (Nos. 91123011, 90923041, 31070742), the State Key Laboratory of Bioreactor Engineering (No. 2060204), 111 Project (No. B07023), the Shanghai Committee of Science and Technology (No. 11DZ2260600), and National "973 Program" (No. 2010CB933900). Thanks to Lei Chen and Prof. Yun Tang for their help in generating the 3D structure in Scheme 1.

## REFERENCES AND NOTES

- Phan, A. T.; Mergny, J. L. Human Telomeric DNA: G-Quadruplex, i-Motif and Watson-Crick Double Helix. *Nucleic Acids Res.* **2002**, *30*, 4618–4625.
- Gehring, K.; Leroy, J. L.; Gueron, M.; Tetrameric, A. DNA Structure with Protonated Cytosine-Cytosine Base Pairs. *Nature* **1993**, *363*, 561–565.
- Kim, M. Y.; Vankayalapati, H.; Kazuo, S.; Wierzba, K.; Hurley, L. H. Telomestatin, a Potent Telomerase Inhibitor That Interacts Quite Specifically with the Human Telomeric Intramolecular G-Quadruplex. *J. Am. Chem. Soc.* **2002**, *124*, 2098–2099.
- Rosu, F.; Gabelica, V.; Shin-ya, K.; De Pauw, E. Telomestatin-Induced Stabilization of the Human Telomeric DNA Quadruplex Monitored by Electrospray Mass Spectrometry. *Chem. Commun.* **2003**, 2702–2703.
- Balasubramanian, S.; Neidle, S. G-Quadruplex Nucleic Acids as Therapeutic Targets. *Curr. Opin. Chem. Biol.* **2009**, *13*, 345–353.
- Gueron, M.; Leroy, J. L. The i-Motif in Nucleic Acids. *Curr. Opin. Struct. Biol.* **2000**, *10*, 326–331.
- Guo, K.; Pourpak, A.; Beetz-Rogers, K.; Gokhale, V.; Sun, D.; Hurley, L. H. Formation of Pseudosymmetrical G-Quadruplex and i-Motif Structures in the Proximal Promoter Region of the RET Oncogene. *J. Am. Chem. Soc.* **2007**, *129*, 10220–10228.
- Brooks, T. A.; Kendrick, S.; Hurley, L. Making Sense of G-Quadruplex and I-Motif Functions in Oncogene Promoters. *FEBS J.* **2010**, *277*, 3459–3469.
- Han, H. Y.; Hurley, L. H. G-Quadruplex DNA: a Potential Target for Anti-cancer Drug Design. *Trends Pharmacol. Sci.* **2000**, *21*, 136–142.
- Fedoroff, O. Y.; Rangan, A.; Chemeris, V. V.; Hurley, L. H. Cationic Porphyrins Promote the Formation of i-Motif DNA and Bind Peripherally by a Nonintercalative Mechanism. *Biochemistry* **2000**, *39*, 15083–15090.
- Alberti, P.; Ren, J. S.; Teulade-Fichou, M. P.; Guittat, L.; Riou, J. F.; Chaires, J. B.; Helene, C.; Vigneron, J. P.; Lehn, J. M.; Mergny, J. L. Interaction of an Acridine Dimer with DNA Quadruplex Structures. *J. Biomol. Struct. Dyn.* **2001**, *19*, 505–513.
- Teulade-Fichou, M. P.; Carrasco, C.; Guittat, L.; Bailly, C.; Alberti, P.; Mergny, J. L.; David, A.; Lehn, J. M.; Wilson, W. D. Selective Recognition of G-quadruplex Telomeric DNA by a Bis(quinacridine) Macrocycle. *J. Am. Chem. Soc.* **2003**, *125*, 4732–4740.
- Li, X.; Peng, Y. H.; Ren, J. S.; Qu, X. G. Carboxyl-Modified Single-Walled Carbon Nanotubes Selectively Induce Human Telomeric i-Motif Formation. *Proc. Natl. Acad. Sci. U. S. A.* **2006**, *103*, 19658–19663.
- Cowan, J. A. Chemical Nucleases. *Curr. Opin. Chem. Biol.* **2001**, *5*, 634–642.
- Zhang, J.; Yang, H.; Shen, G.; Cheng, P.; Zhang, J.; Guo, S. Reduction of Graphene Oxide via L-ascorbic Acid. *Chem. Commun.* **2010**, *46*, 1112–1114.
- Ren, H.; Wang, C.; Zhang, J.; Zhou, X.; Xu, D.; Zheng, J.; Guo, S.; Zhang, J. DNA DNA Cleavage System of Nanosized Graphene Oxide Sheets and Copper Ions. *ACS Nano* **2010**, *4*, 7169–7174.
- Zheng, B.; Wang, C.; Wu, C.; Zhou, X.; Lin, M.; Wu, X.; Xin, X.; Chen, X.; Xu, L.; Liu, H.; et al. Nuclease Activity and Cytotoxicity Enhancement of the DNA Intercalators via Graphene Oxide. *J. Phys. Chem. C* **2012**, *116*, 15839–15846.
- Zhou, X.; Zhang, Y.; Wang, C.; Wu, X.; Yang, Y.; Zheng, B.; Wu, H.; Guo, S.; Zhang, J. Photo-Fenton Reaction of Graphene Oxide: A New Strategy to Prepare Graphene Quantum Dots for DNA Cleavage. *ACS Nano* **2012**, *8*, 6592–6599.
- Wu, J.; Pisula, W.; Mullen, K. Graphenes as Potential Material for Electronics. *Chem. Rev.* **2007**, *107*, 718–747.
- Zhu, S.; Zhang, J.; Qiao, C.; Tang, S.; Li, Y.; Yuan, W.; Li, B.; Tian, L.; Liu, F.; Hu, R.; et al. Strongly Green-Photoluminescent Graphene Quantum Dots for Bioimaging Applications. *Chem. Commun.* **2011**, *47*, 6858–6860.
- Robinson, J. T.; Tabakman, S. M.; Liang, Y.; Wang, H.; Casalongue, H. S.; Vinh, D.; Dai, H. Ultrasmall Reduced Graphene Oxide with High Near-Infrared Absorbance for Photothermal Therapy. *J. Am. Chem. Soc.* **2011**, *133*, 6825–6831.
- Phan, A. T.; Guéron, M.; Leroy, J.-L. The Solution Structure and Internal Motions of a Fragment of the Cytidine-Rich Strand of the Human Telomere. *J. Mol. Biol.* **2000**, *299*, 123–144.
- Sun, D.; Hurley, L. H. The Importance of Negative Superhelicity in Inducing the Formation of G-Quadruplex and i-Motif Structures in the c-Myc Promoter: Implications for Drug Targeting and Control of Gene Expression. *J. Med. Chem.* **2009**, *52*, 2863–2874.
- Li, W.; Wu, P.; Ohmichi, T.; Sugimoto, N. Characterization and Thermodynamic Properties of Quadruplex/Duplex Competition. *FEBS Lett.* **2002**, *526*, 77–81.
- Jin, K. S.; Shin, S. R.; Ahn, B.; Rho, Y.; Kim, S. J.; Ree, M. pH-Dependent Structures of an i-Motif DNA in Solution. *J. Phys. Chem. B* **2009**, *113*, 1852–1856.
- Mergny, J.-L.; Lacroix, L.; Han, X.; Leroy, J.-L.; Helene, C. Intramolecular Folding of Pyrimidine Oligodeoxynucleotides into an i-DNA Motif. *J. Am. Chem. Soc.* **1995**, *117*, 8887–8898.
- Jin, K. S.; Shin, S. R.; Ahn, B.; Jin, S.; Rho, L.; Kim, H.; Kim, S. J.; Ree, M. Effect of C-60 Fullerene on the Duplex Formation of i-Motif DNA with Complementary DNA in Solution. *J. Phys. Chem. B* **2010**, *114*, 4783–4788.
- Ward, D. C.; Reich, E.; Stryer, L. Fluorescence Studies of Nucleotides and Polynucleotides. *J. Biol. Chem.* **1969**, *244*, 1228–1237.
- Kimura, T.; Kawai, K.; Fujitsuka, M.; Majima, T. Fluorescence Properties of 2-Aminopurine in Human Telomeric DNA. *Chem. Commun.* **2004**, 1438–1439.
- Rosu, F.; De Pauw, E.; Guittat, L.; Alberti, P.; Lacroix, L.; Mailliet, P.; Riou, J. F.; Mergny, J. L. Selective Interaction of Ethidium Derivatives with Quadruplexes: An Equilibrium Dialysis and Electrospray Ionization Mass Spectrometry Analysis. *Biochemistry* **2003**, *42*, 10361–10371.
- Monchaud, D.; Allain, C.; Teulade-Fichou, M. P. Thiazole Orange: A Useful Probe for Fluorescence Sensing of G-Quadruplex-Ligand Interactions. *Nucleosides, Nucleotides Nucleic Acids* **2007**, *26*, 1585–1588.
- Lu, C.-H.; Yang, H.-H.; Zhu, C.-L.; Chen, X.; Chen, G.-N.; Graphene, A. *Platform Sensing Biomol.* **2009**, *48*, 4785–4787.
- Kanaori, K.; Sakamoto, S.; Yoshida, H.; Guga, P.; Stec, W.; Tajima, K.; Makino, K. Effect of Phosphorothioate Chirality on i-Motif Structure and Stability. *Biochemistry* **2004**, *43*, 5672–5679.
- Brazier, J. A.; Fisher, J.; Cosstick, R. Stabilization of the DNA i-Motif Structure by Incorporation of 3'-S-Phosphorothioate Linkages. *Angew. Chem., Int. Ed.* **2006**, *45*, 114–117.
- Dai, J. X.; Ambrus, A.; Hurley, L. H.; Yang, D. Z. A Direct and Nondestructive Approach to Determine the Folding Structure of the i-Motif DNA Secondary Structure by NMR. *J. Am. Chem. Soc.* **2009**, *131*, 6102–6104.
- Leroy, J. L. The Formation Pathway of i-Motif Tetramers. *Nucleic Acids Res.* **2009**, *37*, 4127–4134.